PERGAMON

International Journal of Multiphase Flow 28 (2002) 363–384

International Journal of Multiphase Flow

www.elsevier.com/locate/ijmulflow

Correlation of entrainment for annular flow in vertical pipes

Lei Pan, Thomas J. Hanratty *

Department of Chemical Engineering, University of Illinois, 600 South Mathews Avenue, Urbana, IL 61801, USA

Received 11 January 2001; received in revised form 1 June 2001; accepted 3 October 2001

Abstract

A correlation for entrainment in vertical gas–liquid annular flows is presented. The experiments cover pipe diameters of 1.06–5.72 cm, superficial gas velocities of 20–119 m/s, superficial liquid velocities of 0.012–1.35 m/s, gas densities of 0.27–35 kg/m^3 and surface tensions of 0.01–0.073 N/m. Entrainment is considered to result from a balance between the rate of atomization of the wall layer and the rate of deposition of drops. Both rates decrease with increasing liquid flow. A simplified approach which uses the rate equations for low liquid inputs is adopted. The basic idea is that decreases in the rates compensate one another. An approximate empirical equation is obtained by simply substituting the gas velocity for the ratio of the deposition constant and the slip coefficient of the drops. A theoretical approach which relates the deposition constant to particle turbulence is also explored.

Keywords: Gas–liquid pipe flow; Annular flow; Entrainment; Vertical configuration; Rate of atomization; Rate of deposition

1. Introduction

In annular gas–liquid flows part of the liquid moves along the wall as a film and part, as entrained drops. A central problem in understanding the behavior of this system is the prediction of entrainment, E, defined as the ratio of the mass flow of drops, W_{LE}, to the total mass flow of liquid, W_L. A knowledge of this parameter provides the opportunity to develop more sound correlations of liquid holdup and of frictional pressure loss.

* Corresponding author. Tel.: +1-217-333-1318; fax: +1-217-333-5052.
E-mail address: hanratty@scs.uiuc.edu (T.J. Hanratty).

0301-9322/02/$ - see front matter
PII: S0301-9322(01)00073-8

An important concept in understanding the effect of liquid flow on entrainment is the existence of a critical film flow, W_{LFC}, below which entrainment cannot occur (Hewitt and Hall-Taylor, 1970; Dallman et al., 1979; Asali et al., 1985b; Andreussi et al., 1985; Owen, 1986; Willetts, 1987; Schadel et al., 1990). Thus, in an adiabatic system, all of the liquid is not entrained at high gas velocities. An attractive theoretical approach to predict E is to represent it as resulting from a balance between the rate of atomization of liquid layer, R_A, and the rate of deposition of drops, R_D. Reviews of work in this direction are found in the book by Hewitt and Hall-Taylor (1970) and in a recent paper by Dykhno and Hanratty (1996).

This paper provides an assessment of how this approach can be used to develop correlations of measurements of entrainment for liquids with viscosities close to that of water. Recent studies by Lopez de Bertodano et al. (1997, 1998), results in an overlooked thesis by Willetts (1987), and recent theoretical work on the rate of deposition (Hanratty et al., 1999) are used. The proposals are not considered to be final because our understanding of the fundamental rate processes is incomplete. An important aspect of this paper is that the influences of surface tension, gas density, pipe diameter and gas velocity are systematically examined.

The rate of deposition is usually defined as being linearly dependent on the concentration of drops, C, in the units of mass/volume, so that

$$R_D = k_D C = k_D \left(\frac{W_{LE}}{Q_G S} \right). \tag{1}$$

Here, Q_G is the volumeteric flow of the gas and S is the ratio of the drop velocity to the gas velocity. Under equilibrium conditions, where $R_A = R_D$,

$$E = R_A \frac{Q_G S}{k_D W_L}. \tag{2}$$

Dallman et al. (1979) suggested a linear relation for the rate of atomization,

$$\frac{R_A}{U_G (\rho_G \rho_L)^{0.5}} = k_A U_G^n \left(\frac{W_{LF} - W_{LFC}}{P} \right), \tag{3}$$

where W_{LF} is the mass flow of liquid in the film and P is the pipe perimeter.

Under fully developed conditions, Eqs. (1) and (3) give the following relation for E:

$$\frac{E/E_M}{1 - (E/E_M)} = \frac{k_A D U_G^{n+2} S (\rho_G \rho_L)^{0.5}}{4 k_D}, \tag{4}$$

where

$$E_M = 1 - \frac{W_{LFC}}{W_L}. \tag{5}$$

The original notion in developing Eq. (4) was that k_A and k_D would be independent of liquid flow. This implies that (E/E_M) is independent of W_L and that the influence of W_L on E is through Eq. (5). However, measurements of R_A and R_D reveal that both k_A and k_D decrease with W_L at large W_L (Andreussi and Azzopardi, 1983; Hay et al., 1996; Schadel et al., 1990; Govan et al., 1988).

This paper is a continuation of the work of Dykhno and Hanratty (1996) in that it uses Eq. (4) as a guideline to correlate results on entrainment. Simplifying assumptions are made to obtain an approximate relation that will be used to examine the available experimental results. One of these is that, for a fixed gas velocity, k_A/k_D is a constant, equal to the value determined in the limit of $W_L \to O$. The implication is that decreases of k_D with increasing W_L are approximately balanced by decreases in k_A.

There are inconsistencies in the choice of n in Eq. (3). Dallman et al. (1979) suggested $n = 1$ from a consideration of entrainment results in pipes with diameters of 0.95 and 1.20 cm. Measurements of k_A at small droplet concentrations in larger pipes (Schadel et al., 1990) appear to be correlated better with $n = 0$. However, these studies were not carried out over a large enough range of conditions to be conclusive. This paper uses $n = 1$, since the influence of gas velocity on E is better captured and since constants used in the correlating equations become dimensionless.

Theoretical work, which suggests that atomization occurs by a Kelvin–Helmoltz instability, shows that R_A should increase with decreasing surface tension (Schadel and Hanratty, 1989). This is confirmed by measurements which explore the effect of surface tension on entrainment (Willetts, 1987; Whalley et al., 1973; Minh and Huyghe, 1965; Dykhno and Hanratty, 1996). Definitive studies were carried out by Lopez de Bertodano et al. (1997) and Assad et al. (1998) who used Eq. (3) with $n = 1$ and $k_A = k'_A/\sigma$, where σ is the surface tension. Thus,

$$R_A = \frac{k'_A U_G^2 (\rho_G \rho_L)^{0.5}}{\sigma} \quad \frac{(W_{LF} - W_{LFC})}{P}, \tag{6}$$

where k'_A is a dimensionless constant. Eq. (4) can be rewritten as

$$\frac{E/E_M}{1 - (E/E_M)} = \frac{k'_A D U_G^3 S (\rho_G \rho_L)^{0.5}}{4 k_D \sigma}, \tag{7}$$

where k_D has the units of velocity. This equation can be used to examine the effects of pipe diameter, gas velocity, gas density, and surface tension on entrainment. Eq. (7) requires that W_{LF} and U_G are above the critical values of W_{LFC} and U_{GC} that are needed for atomization to occur, so $E = 0$ if $U_G < U_{GC}$ or $W_{LF} < W_{LFC}$. An alternate form of Eq. (7) that includes the notion of a critical gas velocity is the following:

$$\frac{E/E_M}{1 - (E/E_M)} = \frac{k'_A D (U_G - U_{GC})^2 U_G S (\rho_G \rho_L)^{0.5}}{4 k_D \sigma}. \tag{8}$$

This equation implies that $(U_G - U_{GC})^2$ should be substituted for U_G^2 in (6).

Section 2 of this paper summarizes experimental studies and presents an empirical relation for entrainment which simply substitutes U_G for k_D/S in Eq. (8). Section 3 develops a theoretical relation for k_D and uses this, along with Eq. (8), to interpret results for air–water flow in pipes with diameters of 0.953–4.2 cm. Measurements in small diameter pipes (about 1 cm) are the chief source of information about the effects of ρ_G and of σ. Results on entrainment obtained in small and large diameter pipes are consistent with one another. However, measurements of R_A and R_D show distinct differences which are not understood. This matter is discussed in an Appendix A to this paper.

2. Experimental results

2.1. General approach to correlate data

Table 1 summarizes the experiments that are analyzed. Only liquids with viscosities close to water are considered. Thus, all but one of the studies used a liquid with $\mu_L \cong 1$ mPs and a gas with $\mu_G \cong 0.0183$ mPs. The exception is freon–freon, for which $\mu_L = 0.33$ mPs and $\mu_G \cong 0.0123$ mPs. The experiments cover pipe diameters of 0.953–5.72 cm, superficial gas velocities of 20–119 m/s, superficial liquid velocities of 0.012–1.35 m/s, gas densities of 0.27–35 kg/m^3, and surface tensions of 0.01–0.073 N/m (Willetts, 1987; Schadel, 1988; Binder, 1991; Lopez de Bertodano and Jan, 1998; Andreussi and Zanelli, 1976, 1979). The influence of the system variables is studied by using Eq. (8) with the gas velocity, U_G, substituted for k_D/S. Thus,

$$\frac{E}{E_M} = f\left[\frac{(U_G - U_{GC})^2 D(\rho_G \rho_L)^{0.5}}{\sigma}\right], \tag{9}$$

where the dimensionless group on the right-hand side is a modified Weber number.

All of the results on E were obtained by using measurements of the film flow rate, W_{LF}. The experiments of Asali et al. (1985a,b) for air and water flowing in a 4.2 cm pipe are not included because they used droplet flux measurements. The results obtained by Whalley et al. (1973) for air and water and for air and tricholoroethane flowing in a 3.18 cm pipe are not used because they show values of E which are too high, when compared to other measurements at low gas velocities. The measurements of Willetts (1987) of film flow rates as a function of gas velocity for air–fluoroheptane show a qualitative behavior which is quite different from all the other systems studied by him, so they are not considered.

Studies have been carried out by Asali et al. (1985b) with air and water–glycerine solutions with viscosities of 2.59 and 4.6 cP. They provide useful data on the critical flow rate of the film.

Table 1
Summary of experiments

	Fluids	U_{SG} (m/s)	U_{SL} (cm/s)	D (cm)	ρ_G (kg/m^3)	ρ_L (kg/m^3)
Schadel et al. (1990)	Air–water	32–116	1.8–10.4	2.54	1.4	1000
		20–72	1.5–6.7	4.2	1.54	
Binder (1991)	Air–water	25–50	1.2–3.7	5.72	1.6	1000
Lopez de Bertodano	Air–water	25–126	7.4–53.7	0.953	1.6	1000
and Jan (1998);		17–119	7.4–135.0		2.8	
Lopez de Bertodano		14–90	7.4–24.1		4.4	
et al. (1997, 1998)	Freon–freon	4–25	5.0–34.6	1.00	22–35	1400
Willetts (1987)	Air–water	34–67	2.0–14.0	1.026	1.83	998
	Helium–water	52–77	2.0–14.0	1.026	0.27	998
	Air–Genklene	10–50	1.5–12.2	1.026	2.41	1310
Andreussi and Zanelli (1976, 1979) (downflow)	Air–water	5–70	3.7–29.5	2.4	1.38	1000

However, plots of W_{LF} versus the gas velocity for different liquid flows show unrealistic results, in that extrapolations to U_{GC} produce values of W_{LF} which are smaller than W_L. This suggests that much of the liquid entrained in the air exists as a fine mist which does not, readily, deposit. This behavior is observed to a lesser extent in the air/aqueous sulfolane data of Willetts, for which the liquid viscosity is 3.25 cP. Furthermore, the wave structure on viscous liquids can be quite different from what is found for water, in that no disturbance waves appear. We are not in a position to examine the effects of liquid viscosity without having more experimental results. As a consequence, only liquids with viscosities close to water are considered.

The only set of data for a downward configuration, that is considered, was obtained by Andreussi and Zanelli (1976, 1979) for air and water flowing in a 2.4 cm pipe.

The evaluation of E and E_M needs information on W_{LFC} and on U_{GC}. Definitive relations for these quantities are not available. In this paper measurements of the initiation of disturbance waves by Andreussi et al. (1985) were used to obtain W_{LFC}. The plots by Willetts (1987) of W_{LF} versus U_G for fixed liquid mass flow, W_L, provide easily identified critical gas velocities above which $W_L > W_{LF}$. His results are fitted approximately with the relation

$$\frac{D^{0.5}U_{GC}(\rho_L\rho_G)^{0.25}}{\sigma^{0.5}} \cong 40. \tag{10}$$

Eq. (10) is not considered to be final since it has no obvious theoretical justification.

A summary of critical gas velocities, as estimated from the measurements by Willetts (1987); Wallis (1968); Lopez de Bertodano et al. (1997, 1998); Andreussi and Zanelli (1976, 1979) is summarized in Table 2. All of the studies, with the exception of one, used $\rho_L = 1000$ kg/m^3 and $\sigma = 0.073$ N/m. The air–Genklene is characterized by $\rho_L = 1310$ kg/m^3 and $\sigma = 0.025$ N/m. Values of $X_E = D^{0.5}U_{GC}(\rho_L\rho_G)^{0.25}\sigma^{-0.5}$ are also presented. There seems to be a systematic variation

Table 2
Critical gas velocities

Author	Fluids	D (cm)	ρ_G (kg/m^3)	U_{GC} (m/s)	XE
Willetts (1987)	Air–water	1.026	1.83	22	53
	He–water	1.026	0.27	35	53
	Air–Genklene	1.026	2.41	8	39
Wallis (1968)	Air–water (1 atm)	1.588	1.5 (assumed)	18	53
	Air–water (2 atm)	1.588	3.0 (assumed)	12	42
	Air–water (3 atm)	1.588	4.5 (assumed)	11	41
	Air–water (4 atm)	1.588	6.0 (assumed)	10	41
Lopez de Bertodano and Jan (1998)	Air–water	0.953	1.6	24	54
Lopez de Bertodano et al. (1997, 1998)	Air–water	0.953	2.8	15	40
	Air–water	0.953	4.4	13	39
Andreussi and Zanelli (1976, 1979) (downflow)	Air–water	2.4	1.38	11	39

$X_E = D^{0.5}U_{GC}(\rho_G\rho_L)^{0.25}/\sigma^{0.5}$.

of this group with gas density in the data of Lopez de Bertodano and Jan (1998). This suggests that the defining dimensionless group should use $\rho_G^{0.5}$ rather than $(\rho_G\rho_L)^{0.25}$. However, the opposite conclusion would be reached by examining the results of Willetts for air–water and helium–water.

2.2. Effect of W_L

The use of Eq. (9) implies that the effects of liquid flow, W_L, are contained in the definition of E_M, Eq. (5). Clearly, this is an approximation since it is known that k_A and k_D depend on W_L.

Fig. 1 plots values of the entrainment, calculated from measurements of W_{LF}, that were obtained with a tracer technique, by Schadel et al. (1990) for air and water flowing upward in a 4.2 cm pipe at atmospheric conditions. The entrainment, $E = (W_L - W_{LF})/W_L$, is seen to increase with increasing W_L and with increasing U_G.

If the function in Eq. (9) is of the same form as Eq. (8), it would be expected that, at a constant U_G, the entrainment should increase monotonically with increasing W_L, and reach an asymptote at large W_L, where $E_M = 1$. Fig. 1 shows that this type of behavior is only roughly followed and that E, usually, continues to increase at large W_L. This is not surprising since Eq. (8) is obtained by using linear relations for R_A and R_D. It is expected that k'_A/k_D should change with W_L at large values of this quantity. The increase in E suggests that k_D is decreasing with increasing W_L more than is k'_A .

Fig. 1 was constructed by using a value of the critical flow rate in the film of $W_{LFC}/\pi D = 0.085$ kg/ms or $W_{LFC} = 0.0112$ kg/s. For values of $W_L \leqslant W_{LFC}$ all of the liquid should be flowing as a liquid film. It is noted, in Fig. 1, that the lowest values of W_L are close to W_{LFC}.

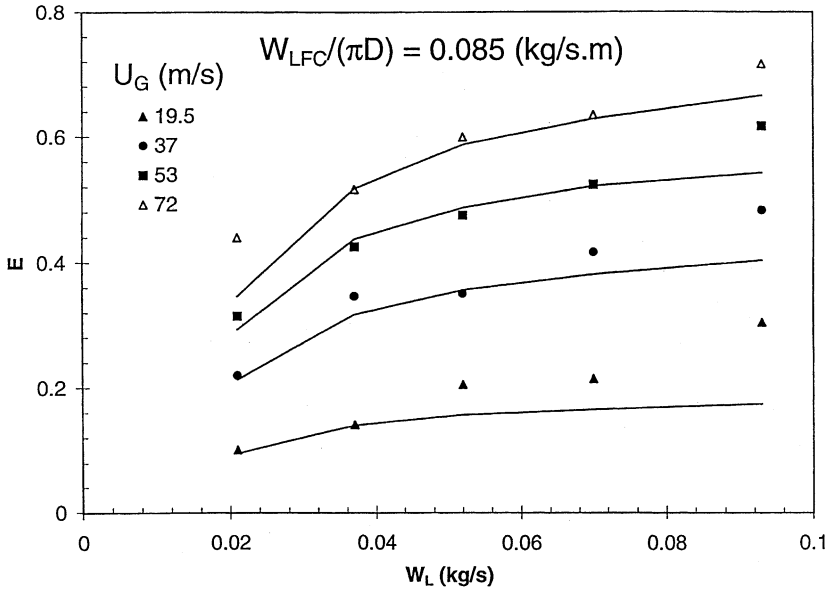

Fig. 1. Measurements of entrainment for air and water flowing up a vertical 4.2 cm pipe. The curves were calculated from values of $\langle E/E_M \rangle$ in Table 3 and Eq. (5).

Consequently, small errors in measuring W_{LF} and W_{LFC} can lead to large errors in the determination of E and E_M. At large values of the gas velocity $E \cong E_M$ so variations of E with W_L reflect the influence of W_L on E_M, as indicated in Eq. (5).

Results for E/E_M, plotted in Fig. 2, indicate that E/E_M is a weak function of W_L and a strong function of U_G. Since measurements of E/E_M at W_L close to W_{LFC} are erratic, results for $W_L < 2W_{LFC}$ are not considered in developing a correlation for E.

2.3. Effect of gas density

All of the measurements show that entrainment increases with increasing gas density. This is illustrated in Fig. 3 where data obtained by Lopez de Bertodano and Jan (1998) for air–water flow for three gas densities and by Willetts (1987) for air–water and helium–water are compared by plotting E/E_M versus $U_G\rho_G^{0.25}$, as suggested by Eq. (9). The measurements extrapolate to the critical gas velocity defined by Eq. (10) and E/E_M varies linearly with $(U_G - U_{GC})$ at small gas velocities.

A first impulse would be to assume entrainment increases with the gas-phase kinetic energy or that E/E_M varies with $\rho_G^{0.5}U_G$. The results in Fig. 3 and results with freon, to be presented later, show that this is not the case.

2.4. Effect of surface tension

All measurements show that entrainment increases with decreasing surface tension. This is illustrated in Fig. 4 for the measurements by Willetts (1987) with air–water and air–genkelene which are, respectively, characterized by surface tensions of 0.073 and 0.026 N/m. The use of a plot of E/E_m versus $U_G\rho_G^{0.25}\sigma^{-0.5}$ approximately captures the effect of surface tension. The

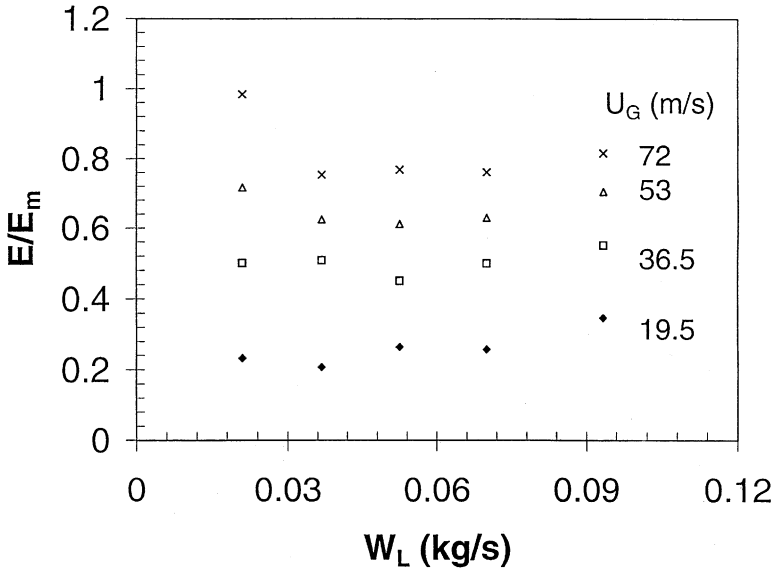

Fig. 2. Plots of E/E_M for air and water flowing up a vertical 4.2 cm pipe.

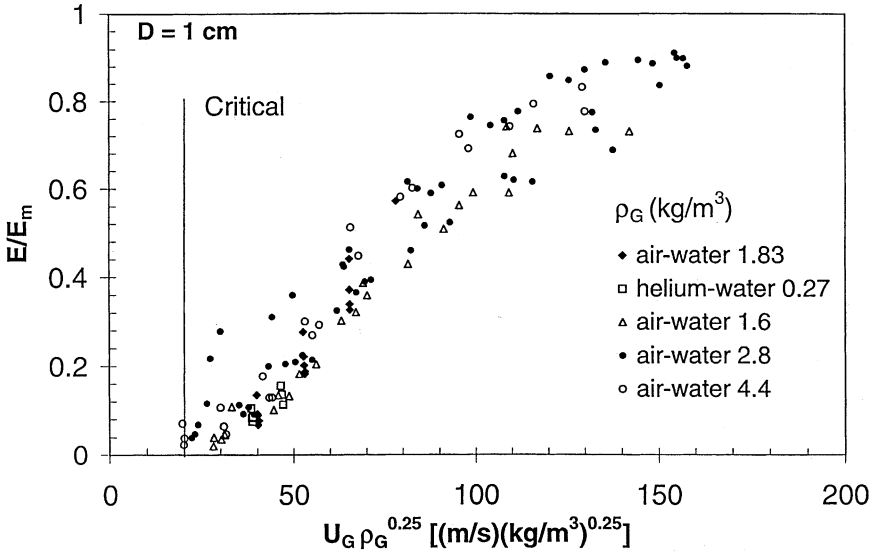

Fig. 3. An examination of the influence of ρ_G on E/E_M. The line on the abscissa represents U_{GC} given by Eq. (10).

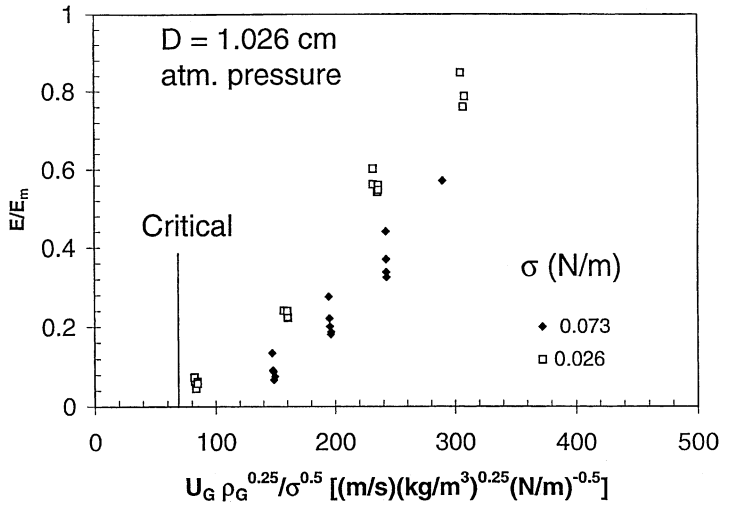

Fig. 4. The effect of surface tension on E/E_M. The line on the abscissa represents U_{GC} given by Eq. (10).

differences seem to reflect the differences in U_{GC} (already documented in Table 3) and not in the slope.

Measurements by Lopez de Bertodano and Jan (1998) for freon ($\rho_G = 22$ to 35 kg/m^3, $\sigma = 0.01$ N/m) and for air–water ($\rho_G = 1.6$ kg/m^3, $\sigma = 0.073$ N/m) are plotted in Fig. 5 as E/E_M versus U_G. The values of U_{GC} calculated with Eq. (10) are indicated on the abscissa. Much larger entrainments are observed for freon, because U_{GC} is smaller and because the sensitivity of E/E_M to changes in gas velocity is larger. For freon, entrainment is initiated at very low gas velocities and

Table 3
Entrainment data for air–water systems

U_G (m/s)	W_L (kg/s)	ρ_G (kg/m^3)	D (m)	$\langle E/E_M \rangle$
32	0.042	1.4	0.0254	0.3091
42	0.042	1.4	0.0254	0.4286
57	0.042	1.4	0.0254	0.6471
69	0.042	1.4	0.0254	0.7002
90.6	0.042	1.4	0.0254	0.792
116	0.042	1.4	0.0254	0.8366
19.5	0.0525	1.53	0.042	0.2192
36.5	0.0525	1.53	0.042	0.4254
53	0.0525	1.53	0.042	0.6123
72	0.0525	1.53	0.042	0.7722
Andreussi and Zanelli (1976, 1979)				
16.5	0.0667	1.38	0.024	0.055
22.4	0.0667	1.38	0.024	0.09
28	0.0667	1.38	0.024	0.1601
33.6	0.0667	1.38	0.024	0.2601
39.7	0.0667	1.38	0.024	0.3902
45.8	0.0667	1.38	0.024	0.4602
50	0.0667	1.38	0.024	0.4902
51.9	0.0667	1.38	0.024	0.5502
58	0.0667	1.38	0.024	0.6402
Lopez de Bertodano and Jan (1998), Lopez de Bertodano et al. (1997, 1998)				
27.1	0.0161	1.5545	0.00953	0.036
43.5	0.0161	1.5787	0.00953	0.1318
62.3	0.0161	1.6189	0.00953	0.3591
85.03	0.0161	1.5787	0.00953	0.563
100	0.0161	1.5545	0.00953	0.7071

increases rapidly with increasing gas velocity, so that a fully entrained condition is reached at a gas velocity for which entrainment is just starting for air–water at atmospheric pressure.

Fig. 6 replots the measurements for the freon system as E/E_M versus $U_G\rho_G^{0.25}\sigma^{-0.5}$, as suggested by Eq. (9). The sets of air–water measurements extrapolate to U_{GC} as E approaches zero. This type of correlation, roughly, brings the two sets of data together. As was found for the air–genkelene system, the measurements for the low surface tension system lie above the measurements for air–water. In both cases, the separation of the data for high and low surface tension fluids is of the order of the accuracy in predicting U_{GC}. The freon–freon measurements show a value of U_{GC} close to zero.

2.5. Effect of pipe diameter/direction of flow

The influence of pipe diameter and the direction of flow can be examined by considering the results obtained for upflow of air and water in 2.5, 4.2 cm pipes by Schadel et al. (1990), in a 0.953 cm pipe by Lopez de Bertodano and Jan (1998), and for downflow in a 2.4 cm pipe by Andreussi

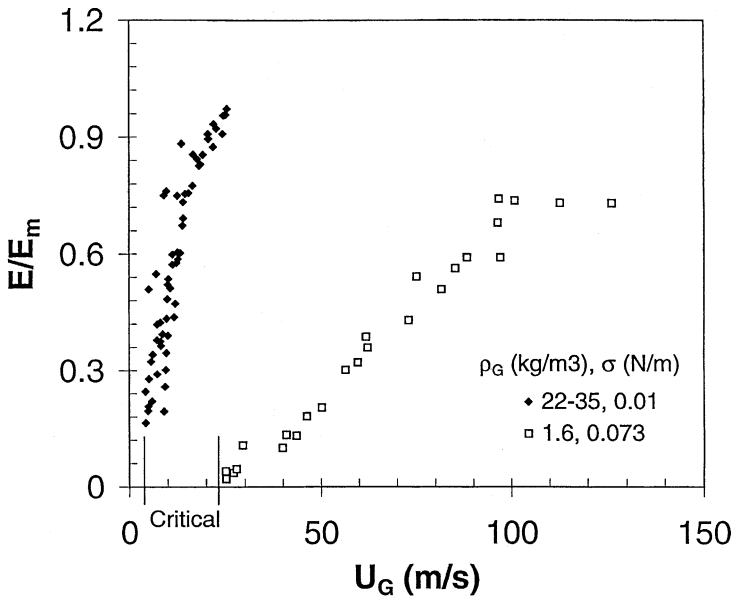

Fig. 5. A comparison of entrainment measurements for freon–freon and air–water in a plot of E/E_M versus U_G ($D = 1$ cm). The lines on the abscissa represent U_{GC} calculated with Eq. (10).

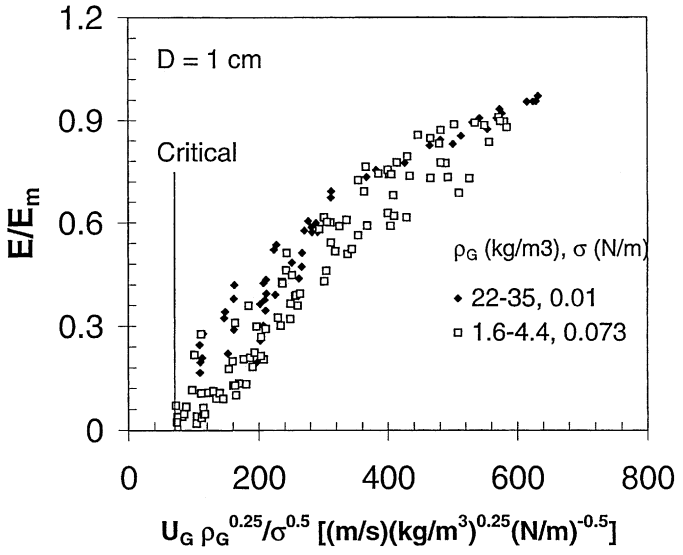

Fig. 6. A comparison of entrainment measurements for freon–freon and air–water in a plot of E/E_M versus $U_G\rho_G^{0.25}/\sigma^{0.5}$ ($D = 1$ cm).

and Zanelli (1976, 1979). The measurements, which show that entrainment increases with pipe diameter, are plotted as E/E_M versus $U_G\rho_G^{0.25}D^{0.5}/\sigma^{0.5}$ in Fig. 7. The spread of the data in the large diameter pipes reflects effects of liquid flow not captured by the linear relations for R_A and R_D. No

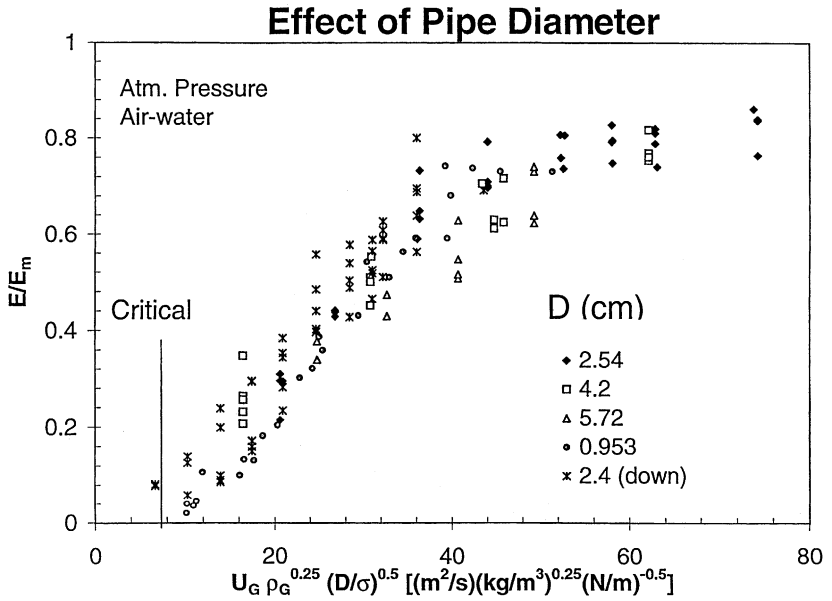

Fig. 7. An examination of the effect of pipe diameter in a plot of E/E_M versus $U_G\rho_G^{0.25}D/\sigma^{0.5}$. The line in the abscissa indicates U_{GC} calculated with Eq. (10) ($D = 0.953$ to 5.72 cm). The line is Eq. (11).

clear-cut differences with flow direction are observed. Eq. (9) roughly represents the effect of pipe diameter.

2.6. Effect of gas velocity

The effect of gas velocity is explored in Fig. 8, which plots entrainment measurements, obtained at atmospheric pressure, in accordance with Eq. (8). The air–water data of Andreussi and Zanelli (1976, 1979), Schadel et al. (1990) and of Lopez de Bertodano and Jan (1998) in 2.4, 2.54, 4.2 and 0.953 cm pipes are considered. The large scatter of the measurements reflects effects of liquid flow not captured by Eq. (8). It is noted that a roughly linear relation can be used to fit the data, so that

$$\frac{E/E_M}{1-(E/E_M)} = A_1 \frac{(U_G - U_{GC})^2(\rho_G\rho_L)^{0.5}D}{\sigma} \tag{11}$$

with $A_1 = 6 \times 10^{-5}$.

3. Theoretical approach

3.1. Outline of the theory

Measurements of liquid interchange between the core of an annular flow and the wall film have been made with a tracer technique for air and water flowing upward in 2.54, 4.2 and 5.7 cm pipes

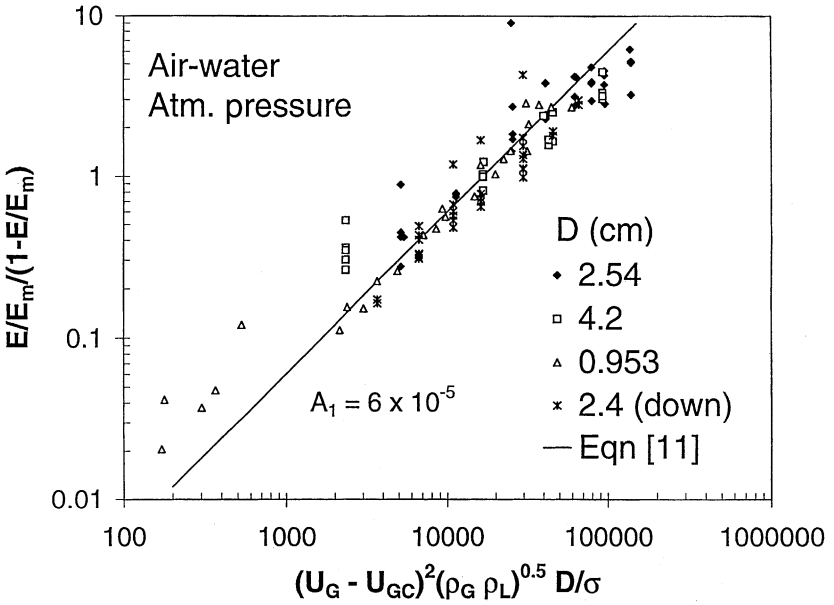

Fig. 8. An examination of the effect of gas velocity in a plot of $E/E_M/(1-E/E_M)$ versus $(U_G-U_{GC})^2(\rho_G\rho_L)^{0.5}D/\sigma$.

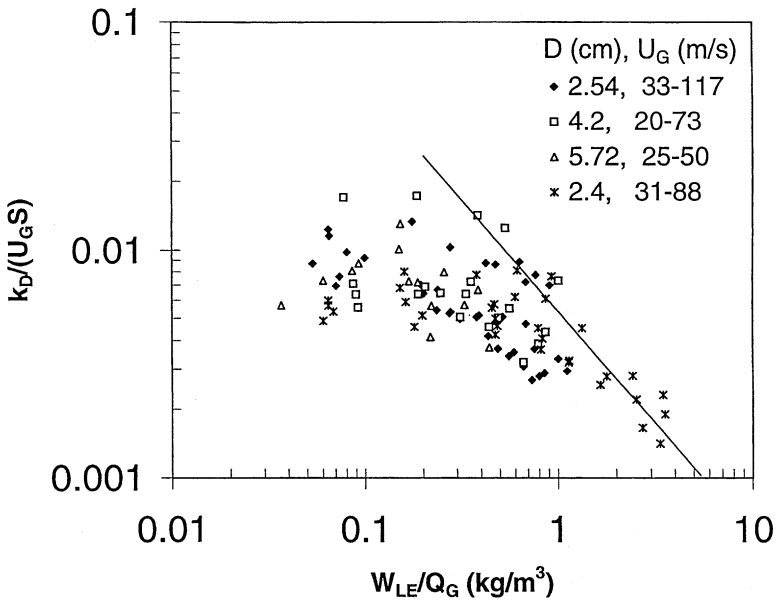

Fig. 9. Measurements of k_D/U_GS for air–water, for $D=2.54$, 4.02, 5.72 cm in an upflow and for $D=2.54$ cm in a downflow. The straight line represents $R_D=$ constant.

(Schadel et al., 1990) and for air and water flowing downward in a 2.4 cm pipe (Andreussi and Zanelli, 1976). These are used to create the plot of k_D/U_GS shown in Fig. 9. For small concen-

trations $k_D \cong 0.009 U_G S$. At large concentrations a nonlinear behavior is observed for which k_D decreases with increasing concentration. At very large concentrations the results approach a situation represented by a line in Fig. 9 that is defined by $k_D \sim C^{-1}$. As shown in Appendix A.1, similar behavior is observed for R_A and R_D. The rate constants k'_A and k_D, thus, decrease with increasing W_L. For very large W_L, a situation is approached for which both R_A and R_D are constants. A discussion of possible causes for the influence of drop concentration on k_D is presented by Hay et al. (1996).

Progress in developing a theoretical understanding of k_D is summarized in a recent paper by Hanratty et al. (1999). The rate of deposition on the wall can be represented as

$$R_D = V_W C_W, \tag{12}$$

where C_W is the concentration of drops at the wall and V_W is the mean velocity of drops toward the wall. If the velocity fluctuations of the drops are described by a Gaussian distribution

$$V_W = (\overline{v_p^2})^{0.5}/(2\pi)^{0.5}, \tag{13}$$

where $\overline{v_p^2}$ is the mean-square of the velocity fluctuations of the drops in a direction perpendicular to the wall. Furthermore, measurements of droplet concentrations in the gas phase (Hay et al., 1996) show that the profile characterizing the spatial distribution is flat under fully developed conditions. Therefore, the concentration at the wall is the bulk concentration, so that

$$k_D = (\overline{v_p^2})^{0.5}/(2\pi)^{0.5}. \tag{14}$$

Lee et al. (1989) have shown that the mean-square of the turbulent velocity fluctuations of drops in dilute concentrations is given as

$$\overline{v_{p_o}^2} = \frac{\beta\tau_{LF}}{0.7 + \beta\tau_{LF}}\overline{v_G^2}, \tag{15}$$

where the mean-square of the turbulent velocity fluctuation of the gas, $\overline{v_G^2}$, can be approximated by

$$\overline{v_G^2} = (0.9 v^*)^2 \tag{16}$$

and v^* is the friction velocity of the gas. The Lagrangian time scale of the fluid, τ_{LF}, and the reciprocal of the inertial time constant of the particles, β, are given as

$$\tau_{LF} = \frac{0.046 D}{v^*}, \tag{17}$$

$$\beta = \frac{3 C_D \rho_G u_S}{4 d \rho_P}, \tag{18}$$

where C_D is the drag-coefficient u_S, the slip velocity and d, the drop diameter.

The measurements represented by Eq. (15) were carried out under conditions that the droplets were in the turbulent field long enough that they had come to equilibrium with the gas-phase turbulence. This condition might not be met in small diameter pipes and at small gas velocities (large drop sizes).

The estimation of $\overline{v_p^2}$ requires the determination of β. For this purpose, the slip velocity was set equal to the terminal velocity

$$u_T = \left(\frac{4dg(\rho_L - \rho_G)}{3C_D\rho_G} \right)^{0.5}. \tag{19}$$

A droplet Reynolds number is defined as

$$Re_p = \frac{\rho_G d u_T}{\mu_G} \tag{20}$$

and the drag-coefficient is taken as

$$C_D = \frac{24}{Re_p} \tag{21}$$

for $Re_p < 2$ and as

$$C_D = \frac{18.5}{Re_p^{0.6}} \tag{22}$$

for $2 < Re_p < 500$.

The dropsize was assumed to be given by an upper limit log-normal distribution defined by Tatterson and Hanratty (1977). The Sauter mean diameter, d_{32}, was calculated with a correlation presented by Azzopardi (1985). The normalized volume distribution, defined in Tatterson and Hanratty (1977), is given as

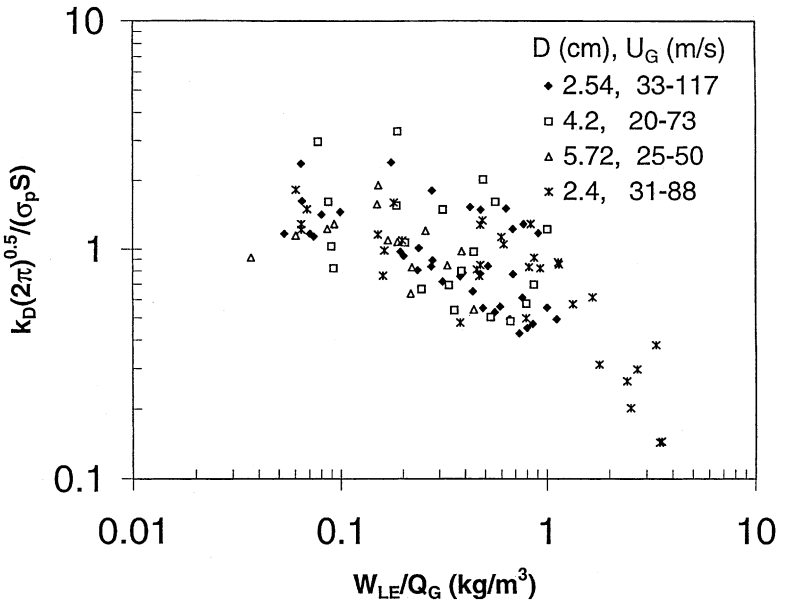

Fig. 10. Plot of $k_D(2\pi)^{0.5}/S(\overline{v_p^2})^{1/2}$ for the data of Zanelli and Andreussi for downflow and for Schadel et al. for upflow in 2.54, 4.02, 5.72 cm pipes.

$$\frac{dV}{dd} = f_V(d), \tag{23}$$

where d designates the drop diameter. The mean β to be used in Eq. (15) is

$$\bar{\beta} = \int_0^{d_m} \left(\frac{3C_D \rho_G u_T}{4 d_p \rho_L} \right) (f_V)\, dd. \tag{24}$$

Fig. 10 presents plots of $k_D(2\pi)^{0.5}/S(\overline{v_p^2})^{0.5}$ versus the concentration, W_{LE}/Q_G. The slip ratio S was set equal to unity. For conditions in which the drops are in the field long enough that a stationary state has been reached, $k_D(2\pi)^{0.5}/(\overline{v_p^2})^{0.5}$ should be approximately equal to unity. Considering the accuracy of the experiments and of the calculations, grudging support is given to the theoretical calculations of k_D for dilute concentrations. However, the results in the 2.54 cm pipe at the two lowest gas velocities, 33 and 43 m/s, are significantly higher that the other results. This could suggest that other parameters than fluid turbulence are operative such as the velocity imparted to the drops when they are removed from the film on the wall (Andreussi and Azzopardi, 1983).

3.2. Calculations of entrainment

Results obtained for the rate of atomization and for the rate of deposition document the nonlinearity of these processes in that both k'_A and k_D decrease with increasing liquid flow. The complexity of these results and the inaccuracies associated with the performance of very difficult experiments make it difficult, at present, to proceed directly from the available measurements of R_A and R_D to produce predictive methods for entrainment.

Consequently, a first step would be to explore modest changes in the approach presented in Section 1. The linearized equations for R_A and R_D will be used so that Eq. (8) is the defining equation for entrainment. The implementation of Eq. (8) in Section 2 involved simply the replacement of k_D/S with U_G. Improvements in this approach might be realized by using a more sophisticated representation of k_D that is based on physical reasoning.

Fig. 11 presents calculations of entrainment, with Eq. (8), in which k_D is given by Eq. (14) and the slip ratio, S, is set equal to unity. The particle turbulence $(\overline{v_p^2})^{1/2}$ is calculated with the methods outlined in the previous section. The system considered is air and water flowing upward at atmospheric pressure in pipes with diameters of 0.953, 2.54, 4.2 cm, and flowing downward in a 2.4 cm pipe.

In order to avoid the type scatter shown in Fig. 8, the data points, shown in Fig. 11, are averages of the values of E/E_M, such as those shown in Fig. 2, for a given gas velocity. These are summarized in Table 3 as $\langle E/E_M \rangle$. The validity of representing the data in this way is explored in Fig. 1, where the curves are calculated from the $\langle E/E_M \rangle$ in Table 3 and Eq. (5). The values of W_L listed in Table 3 also represent averages.

A value of $k'_A = 1.4 \times 10^{-6}$ was used to do the calculations. Good agreement is noted between the calculated curves and the data points. Furthermore, it is shown in Appendix A.2 that measurements of R_A in small diameter pipes are about 2/3 of what is found for larger pipes. If $k'_A = 2/3 \times 1.4 \times 10^{-6}$ is used, the calculations for $D = 0.953$ cm are closer to the measurements than those indicated in Fig. 11.

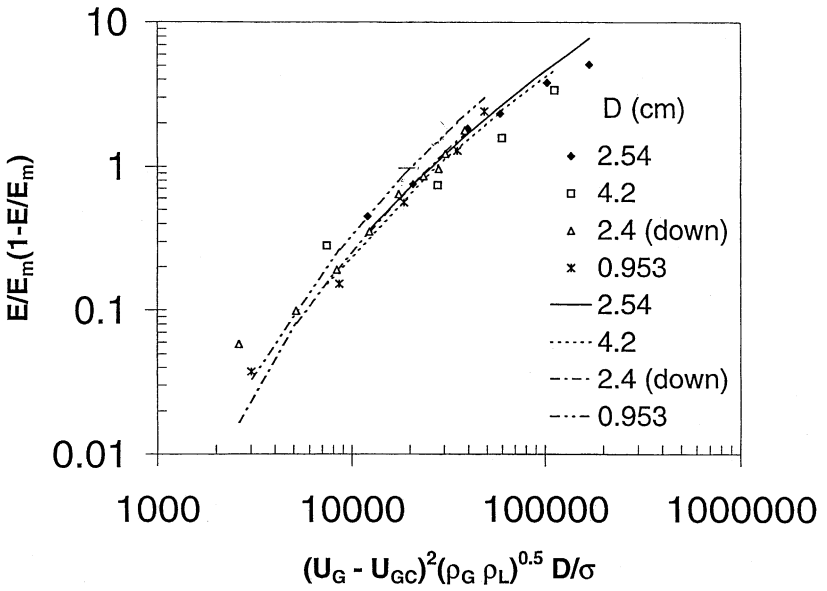

Fig. 11. Plot of $\langle E/E_M\rangle/1-\langle E/E_M\rangle$ versus U_G calculated with Eq. (8) and $k_D=(\overline{v_p^2})^{1/2}/(2\pi)^{1/2}$. Data points are values of $\langle E/E_M\rangle$ listed in Table 3.

4. Discussion

Empirical equation (8) with U_{GC} defined by Eq. (10) and W_{LFC} obtained from Andreussi et al. (1985) provides an approximate correlation for presently available measurements of entrainment for annular flows in vertical pipes for liquids with viscosities close to that of water. One of the concerns is that the effects of fluid properties are determined from experiments in pipes with diameters approximately equal to 1 cm. Clearly, more data are needed with larger diameters and for liquids with larger viscosities. Since wave structures on the wall layer are quite different for high viscosity liquids from what is observed with water one can anticipate that the equation for R_A could be fundamentally different.

An assumption that was made in developing the empirical equation is that k_D/S is proportional to U_G. Measurements of k_D/U_GS presented in Figs. 9 and 14 show that this is a crude assumption. Better results should be obtained by using Eq. (7) and models for k_D and S. For fully developed flows $k_D\sim\sigma_P$, where σ_P is the root-mean square of the velocity fluctuations of the particle in a direction perpendicular to the wall. A method for estimating σ_P is given (in Eqs. (15)–(24)) that requires information on drop size. Despite the uncertainties in predicting drop size, the use of $k_D\sim\sigma_P$ should provide more reliable correlations of entrainment for large diameter pipes than the empirical approach.

Measurements of R_A and R_D for a 1 cm pipe show smaller values than those obtained with pipes that are 2.5 cm or larger (see Appendix A.2). However, the ratio of the rate constants, k'_A/k_D is roughly the same for small and large diameters.

A more difficult task is the prediction of the effects of liquid flow rate. Both k'_A and k_D decrease with increasing liquid flow. The approach taken in this paper depends on the assumption that the

ratio of these two rate constants remains constant. Clearly this is an approximation. An accurate accounting for the effects of liquid flow is a longer range endeavor.

5. Comparison with previous studies

Paleev and Filippovich (1966) suggested that

$$E \sim \frac{\bar{\rho}}{\rho_L}\left(\frac{\mu_L U_G}{\sigma}\right)^2, \tag{25}$$

where $\bar{\rho}$ is the density of the gas–liquid mixture flowing in the core. Wallis (1968) discusses studies which show that the effect of liquid viscosity predicted by Eq. (A.2) is not observed. He, therefore, proposed the following relation:

$$E \sim \left(\frac{U_G \mu_G}{\sigma}\right)^2 \left(\frac{\rho_G}{\rho_L}\right). \tag{26}$$

The gas viscosity was introduced into Eq. (26) in order to produce a nondimensional equation. However, no experimental or theoretical results are available that justify this inclusion.

The empirical equation presented in this paper differs from Eq. (26) in several ways:

1. It allows for the existence of a critical liquid flow rate below which liquid entrainment cannot exist.
2. It predicts weaker effects of surface tension and of gas density.
3. A direct effect of pipe diameter is included.

Ishii and Mishima (1989) proposed the following equation for small entrainments:

$$E \sim \left[\left(\frac{\rho_G U_G^2 D}{\sigma}\right)\left(\frac{\rho_L - \rho_G}{\rho_G}\right)^{1/2}\right]^{1.25} \left(\frac{U_{SL} D \rho_L}{\mu_L}\right)^{0.25}. \tag{27}$$

Again, this equation does not recognize the existence of critical liquid or gas flows and introduces an influence of liquid viscosity which is not warranted. However, there are some strong similarities. The dominant term in Eq. (27) is $(\rho_L \rho_G)^{0.5} U_G^2 D/\sigma$ for $\rho_G \ll \rho_L$. The dominant term in Eq. (9) is $(\rho_G \rho_L)^{0.5}(U_G - U_{GC})^2 D/\sigma$.

Govan et al. (1988) developed an analysis for the entrainment at equilibrium by considering rates of atomization and deposition, R_A and R_D. An important aspect of this work is the introduction of nonlinear effects in the equation for R_D, that is, a decrease in the deposition constant at large drop concentrations. A flaw in their approach is that the influence of nonlinearities on R_A is not considered.

Acknowledgements

This work was supported by the Engineering Research Program of the Office of Basic Energy Sciences of the Department of Energy under grant DOE DEF G02-86ER 13556 and by Shell Technology.

Appendix A

A.1. Rate of atomization in large diameter pipes

Measurements of the liquid interchange between the core of an annular flow and the wall film have been made with the tracer technique for air and water flowing upward in 2.54, 4.2 and 5.7 cm pipes (Schadel et al., 1990) and for air and water flowing downward in a 2.4 cm pipe (Andreussi and Zanelli, 1976). These are plotted in Fig. 12 as R_A versus $[(\rho_G\rho_L)^{0.5}(U_G - U_{GC})^2 (W_{LF} - W_{LFC})/\pi D\sigma]$. The measurements by Andreussi and Zanelli (1976) for downflows are fitted with the equation

$$R_A = 0.30[1 - \exp(-X/460,000)], \tag{A.1}$$

where

$$X = (\rho_G\rho_L)^{0.5}(U_G - U_{GC})^2(W_{LF} - W_{LFC})/\pi D\sigma \tag{A.2}$$

and R_A is given in the units of kg/m^2 s. Note that $(U_G - U_{GC})^2$ has been substituted for U_G in Eq. (6). It is noted that the upflow data lie above the curve representing this equation.

In the limit of small X one obtains

$$R_A = k'_A X \tag{A.3}$$

with $k'_A = 0.66 \times 10^{-6}$ for the measurements of Andreussi and Zanelli. The data of Andreussi and Zanelli most clearly show a nonlinear behavior since larger film flow rates can be sustained in downflows than in upflows. Eq. (A.1) and the data in Fig. 12 indicate a maximum rate of atomization that is reached at large W_{LF}; that is,

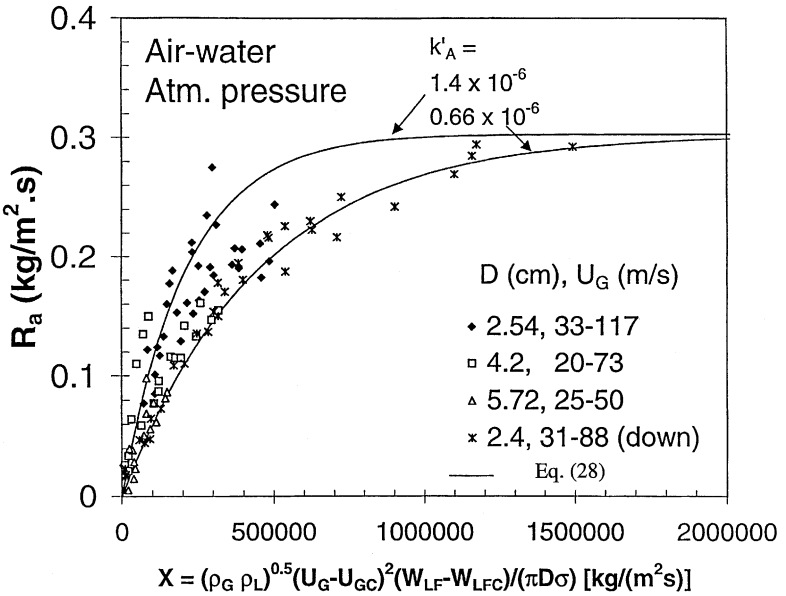

Fig. 12. Measurements of R_A for air–water for $D = 2.54$, 4.2 and 5.72 cm in an upflow and for $D = 2.4$ cm in a downflow. The curves are Eq. (A.1).

$$R_{AM} \cong 0.30 \quad (\mathrm{kg/m^2\ s}) \tag{A.4}$$

as suggested by Dykhno and Hanratty (1996). The constants in Eq. (A.1) have the units of $\mathrm{kg/m^2\ s}$. They may be defined as $R_{AM} = 0.30\ \mathrm{kg/m^2\ s}$ and as $1.53 \times 10^6 R_{AM} = 460,000\ \mathrm{kg/m^2\ s}$. A value of $k'_A = 1.4 \times 10^{-6}$ was used for the calculated values of E presented in Fig. 11. A second curve in Fig. 12 was calculated with an equation of the same form as Eq. (A.1) with $R_{AM} \cong 0.30\ \mathrm{kg/m^2\ s}$ but with a limiting behavior of $R_A = 1.4 \times 10^{-6} X$ for $X \to 0$.

The method for presenting data for R_A in Fig. 12 is very similar to what has been used by the Bertodano research group in several of their papers. The only difference is that $(U_{SG} - U_{GC})^2$ is used instead of U_{SG}^2. This was done so as to accommodate the observed critical gas velocity for entrainment that is shown in Figs. 3–7. However, there is no theoretical justification for doing this. The type of plot used by Bertodano would produce smaller k'_A.

The plots of $k_D/U_G S$, shown in Fig. 9, and of R_A, shown in Fig. 12, are similar. A linear behavior is shown at small liquid flows in that R_A varies linearly with x and k_D is roughly constant. Both show a constancy in R_A and R_D at large liquid flows.

A.2. Rate of atomization and deposition in a small diameter pipe

Measurements of R_A and R_D have been obtained by Lopez de Bertodano and Jan (1998) and Lopez de Bertodano et al. (1997) for air–water flow in a 0.953 cm pipe and for freon–freon flow in a 1.00 cm pipe. A film withdrawal unit was used to measure W_{LF} under conditions that the flow was fully developed. Fig. 13 presents a plot of R_A versus X, where X is defined by Eq. (A.2), for

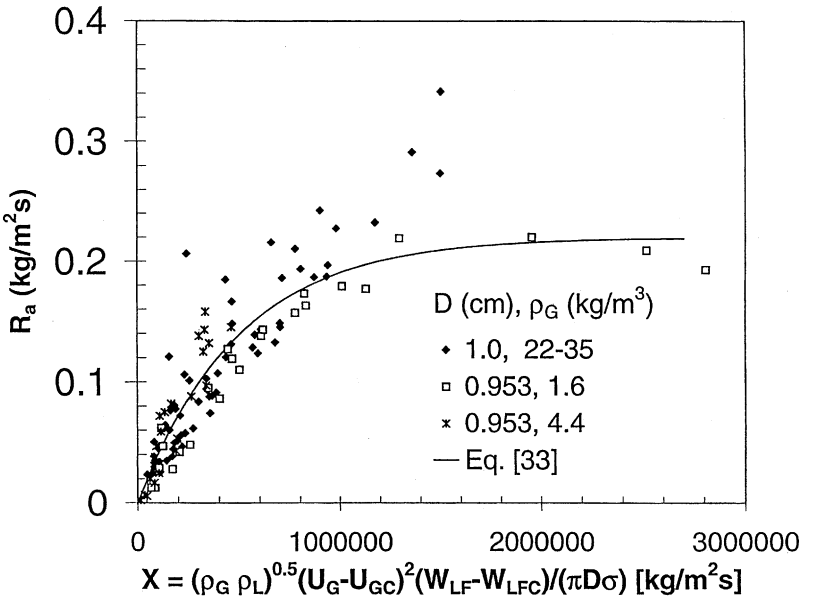

Fig. 13. Plot of R_A versus $(\rho_G \rho_L)^{1/2}(U_G - U_{GC})^2(W_{LF} - W_{LFC})/\pi D\sigma$ for air–water in a 0.953 cm pipe ($\rho_G = 1.6$, 4.4 $\mathrm{kg/m^3}$) and for freon–freon in a 1 cm pipe. The curve represents Eq. (A.1).

air–water flow with $\rho_G = 1.6$ and 4.4 kg/m^3. The limiting slope for small W_{LF} is $k'_A = 0.44 \times 10^{-6}$ and the data for all W_{LF} are fitted reasonably well with the equation

$$R_A = 0.22[1 - \exp(-X/500,000)]. \tag{A.5}$$

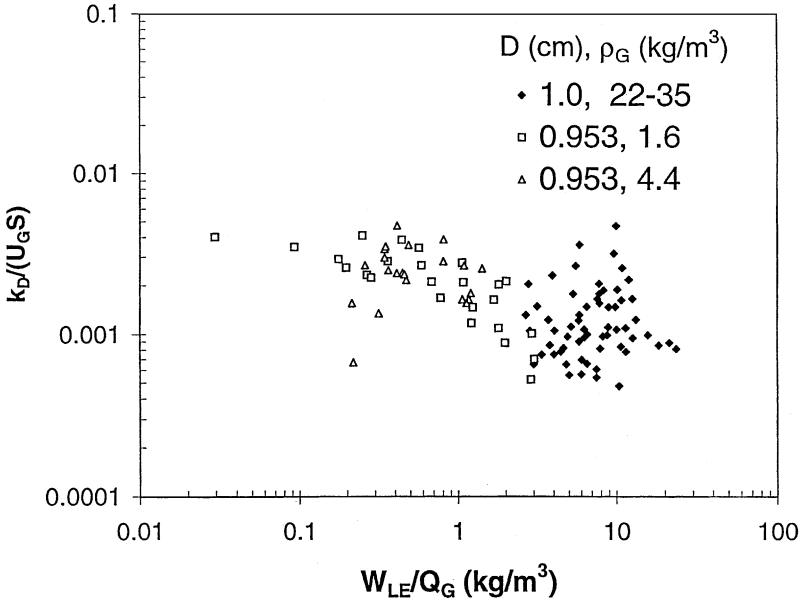

Fig. 14. Plot of k_D/U_G for air–water ($\rho_G = 1.6$, 4.4 kg/m^3) and for freon–freon.

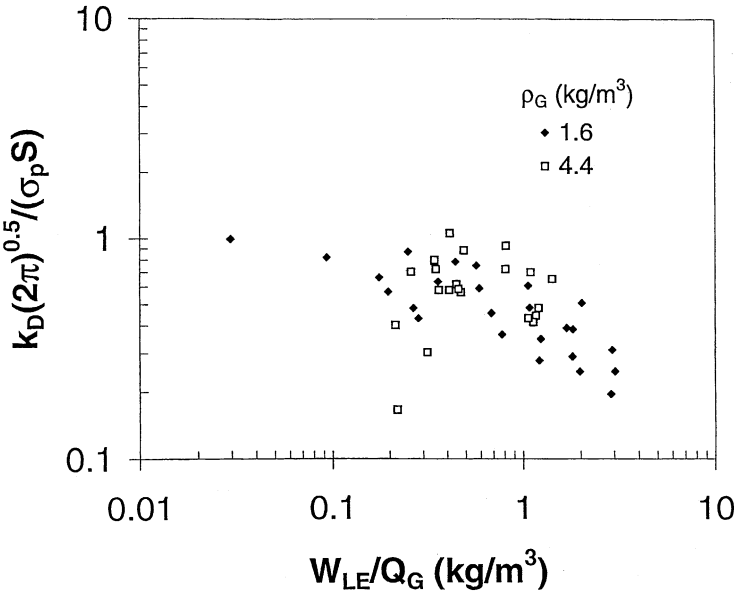

Fig. 15. Plot of $k_D(2\pi)^{0.5}/(\overline{v_p^2})^{1/2}$ for air–water in a 0.953 pipe.

Measurements of R_A obtained for the freon–freon flow are also presented in Fig. 13 as filled diamonds.

Approximate agreement is noted between the measurements with air–water and with freon–freon at small X when the data are plotted in this way, as has already been noted by Lopez de Bertodano et al. (1997). A comparison of these values of R_A with those obtained in pipes with larger pipe diameters reveals that they are smaller than those observed by a factor of about 2/3. The measurements for freon–freon appear to be behaving differently in that they do not show a plateau at large X.

Fig. 14 presents measurements of $k_D/U_G S$ for air–water flow ($\rho_G = 1.6$ kg/m^3 and $\rho_G = 4.4$ kg/m^3) in a 0.953 cm pipe and for freon–freon flow in a 1 cm pipe ($\rho_G = 22$ to 35 kg/m^3). As was found for k'_A, this plot shows smaller k_D/U_G (by factor of ca. 2/3) than that was observed in larger diameter pipes. The large scatter of the freon–freon measurements of k_D is surprising, considering the fact that the data for entrainment (Figs. 5 and 6) are reasonably consistent. This could reflect inaccuracies in the determination of the mass exchange rate for this system. The freon/freon system also differs from the air/water system in that atomization is initiated at much smaller volumetric gas velocities. As a consequence, the concentration of entrained drops is larger and the rate process should be nonlinear.

Values of $k_D(2\pi)^{0.5}/(\overline{v_p^2})^{0.5}$ for air–water flows are presented in Fig. 15. These are approximately equal to unity in the limit of small drop concentrations.

References

Andreussi, P., Asali, J.C., Hanratty, T.J., 1985. Initiation of small waves in gas–liquid flows. AIChE J. 31, 119–126.

Andreussi, P., Azzopardi, B.J., 1983. Droplet deposition and interchange in annular two-phase flow. Int. J. Multiphase Flow 9, 681–697.

Andreussi, P., Zanelli, S., 1976. Liquid phase mass transfer in annular two-phase flow. Ing. Chim. 12, 132–136.

Andreussi, P., Zanelli, S., 1979. Downward annular and annular-mist flow of air–water mixtures. In: Durst, F., Tsiklauri, G.V., Afgan, N.H. (Eds.), Two-Phase Momentum, Heat and Mass Transfer, vol. 2. Hemisphere, Washington, DC.

Asali, J.C., Hanratty, T.J., Andreussi, P., 1985a. Interfacial drag and film height for vertical annular flow. AIChE J. 31, 895–902.

Asali, J.C., Leman, G.W., Hanratty, T.J., 1985b. Entrainment measurements and their use in design equations. Physiochem. Hydrodyn. 6, 207–221.

Assad, A., Jan, C.S., Lopez de Bertodano, M., Beus, S., 1998. Scaled entrainment measurements in ripple–annular flow in a small tube. Nucl. Eng. Des. 184, 437–447.

Azzopardi, B.J., 1985. Drop sizes in annular two-phase flow. Exp. Fluids 3, 53–59.

Binder, J.L., 1991. Use of Lagrangian methods to describe particle deposition and distribution in dispersed flows. Ph.D. Thesis, University of Illinois, Urbana.

Dallman, J.C., Jones, B.G., Hanratty, T.J., 1979. Interpretation of entrainment measurements in annular gas–liquid flow. In: Two-Phase Momentum Heat and Mass Transfer, vol. 2. Hemisphere, Washington, DC, pp. 681–693.

Dykhno, L.A., Hanratty, T.J., 1996. Use of the interchange model to predict entrainment in vertical annular flow. Chem. Eng. Commun. 141–142, 207–235.

Govan, A.H., Hewitt, G.F., Owen, D.G., Bott, T.R., 1988. An improved CHD modeling code. In: Second UK National Conference, Strathchlyde University, Glasgow, pp. 33–52.

Hanratty, T.J., Woods, B.D., Iliopoulos, I., Pan, L., 1999. The roles of interfacial stability and particle dynamics in multiphase flows: a personal viewpoint. Int. J. Multiphase Flow (to be published).

Hay, K.J., Liu, Z.C., Hanratty, T.J., 1996. Relation of deposition to drop size when the rate law is nonlinear. Int. J. Multiphase Flow 22, 829–848.

Hewitt, G.L., Hall-Taylor, N.S., 1970. Annular Two-Phase Flow. Pergamon Press, Oxford.

Ishii, M., Mishima, K., 1989. Droplet entrainment correlation in annular two-phase flow. Int. J. Heat Mass Transfer 32, 1835–1846.

Lee, M.M., Hanratty, T.J., Adrian, R.J., 1989. An axial viewing photographic technique to study turbulence characteristics of particles. Int. J. Multiphase Flow 15, 787–802.

Lopez de Bertodano, M.A., Jan, C.S., 1998. Entrainment data in vertical flows. Private communication.

Lopez de Bertodano, M.A., Jan, C.S., Assad, A., Beus, S., 1998. Entrainment rate of droplets in the ripple–annular regime for small diameter vertical ducts. In: Third International Conference on Multiphase Flow, Lyon, France.

Lopez de Bertodano, M.A., Jan, C.S., Beus, S.G., 1997. Annular flow entrainment rate experiment in a small vertical pipe. Nucl. Eng. Des. 178, 61–70.

Minh, T.-Q., Huyghe, J., 1965. Some hydrodynamic aspects of annular two phase flow. In: Proceedings of Conference in Two-Phase Flow. Exeter, June, paper C2, pp. 21–23.

Owen, D.G., 1986. An experimental and theoretical analysis of equilibrium annular flows. Ph.D. Thesis, University of Birmingham, UK.

Paleev, J.J., Filippovich, B.S., 1966. Phenomena of liquid transfer in two-phase dispersed annular flow. Int. J. Heat Mass Transfer 9, 1089–1093.

Schadel, S.A., 1988. Atomization and deposition rates in vertical annular two-phase flow. Ph.D. Thesis, University of Illinois, Urbana.

Schadel, S.A., Hanratty, T.J., 1989. Interpretation of atomization rates of the liquid film in gas liquid annular flow. Int. J. Multiphase Flow 15, 893–900.

Schadel, S.A., Leman, G.W., Binder, J.L., Hanratty, T.J., 1990. Rates of atomization and deposition in vertical annular flow. Int. J. Multiphase Flow 16, 363–374.

Tatterson, D.F., Dallman, J.C., Hanratty, T.J., 1977. Drop sizes in annular gas–liquid flows. AIChE J. 23, 68–76.

Wallis, G.B., 1968. Phenomena of liquid transfer in two-phase dispersed annular flow. Int. J. Heat Mass Transfer 11, 783–785.

Whalley, P.B., Hewitt, G.F., Hutchison, P., 1973. Experimental wave and entrainment measurements in vertical annular two-phase flow. AERE Report R7521.

Willetts, I., 1987. Non-aqueous annular two-phase flow. Ph.D. Thesis, University of Oxford, UK.